Decentralized control of sound radiation from an aircraft-style panel using iterative loop recovery

N. H. Schiller, R. H. Cabell, and C. R. Fuller

Acoustics'08 Paris
July 4, 2008

A decentralized LQG-based control strategy is designed to reduce low-frequency sound transmission through periodically stiffened panels. While modern control strategies have been used to reduce sound radiation from relatively simple structural acoustic systems, significant implementation issues have to be addressed before these control strategies can be extended to large systems such as the fuselage of an aircraft. For instance, centralized approaches typically require a high level of connectivity and are computationally intensive, while decentralized strategies face stability problems caused by the unmodeled interaction between neighboring control units. Since accurate uncertainty bounds are not known *a priori*, it is difficult to ensure the decentralized control system will be robust without making the controller overly conservative. Therefore an iterative approach is suggested, which utilizes frequency-shaped loop recovery. The approach accounts for modeling error introduced by neighboring control loops, requires no communication between subsystems, and is relatively simple. The control strategy is validated using real-time control experiments performed on a built-up aluminum test structure representative of the fuselage of an aircraft. Experiments demonstrate that the iterative approach is capable of achieving 12 dB peak reductions and a 3.6 dB integrated reduction in radiated sound power from the stiffened panel.

1 Introduction

Interior noise levels in commercial and general aviation aircraft are an occupational hazard for flight crew and an inconvenience for passengers. Since passive treatments, such as poroelastic foam, are not effective at low frequencies due to size and weight constraints, this paper focuses on an active control strategy. In particular, primary structural control is considered. As the name implies, this approach reduces interior noise by applying control inputs directly to the primary structure (e.g., piezoelectric patches bonded to the aircraft sidewall).

Past research has shown that active structural control can be used effectively on laboratory scale systems. However, significant implementation issues have to be addressed before active control can be implemented on a full-scale aircraft [1]. While centralized strategies have been used to simultaneously reduce the sound radiation from multiple aircraft-style bays [2], these strategies require a high level of connectivity, are computationally intensive, and can be sensitive to transducer failures. On the other hand decentralized strategies are simple, computationally efficient, and scalable. Unfortunately the performance of decentralized strategies is often limited due to the interaction between neighboring controllers [2]. The goal of this work is to show that a scalable decentralized control system can be effective when implemented in a simple iterative loop.

This paper begins with a brief description of decentralized control along with a discussion of its limitations. In particular, we demonstrate that the approach is only effective if the local control units are robust to the modeling error introduced by neighboring controllers. While it might be tempting to use inherently robust strategies like direct velocity feedback, the conservative nature of these approaches provides stability guarantees at the expense of performance. Therefore this paper focuses on linear quadratic Gaussian (LQG) control. Since LQG designs can have arbitrarily poor stability margins, frequency shaping and loop transfer recovery (LTR) are often necessary to improve the robust stability and performance of the system. However, both of these techniques assume uncertainty bounds are known *a priori*, which is not always true. Therefore an iterative scheme is presented to account for the lack of *a priori* information. In addition to discussing the control methodology, this paper also describes the experiment that was used to evaluate the proposed approach.

2 Decentralized Control

Decentralized control implies that each control unit is designed and implemented independently, as demonstrated by Fig. 1(a). In this example the plant is defined as

$$G = \begin{bmatrix} G_{11} & G_{12} \\ G_{21} & G_{22} \end{bmatrix} \tag{1}$$

where G_{ij} denotes the transfer function from the ith actuator to the jth sensor. In the context of this work, the diagonal terms of G model the response between actuator/sensor pairs on the same bay, while the off-diagonal terms capture the coupling between actuators and sensors on different bays. Decentralized control is particularly effective if the plant is diagonally dominant (ie $G_{11}G_{22} >> G_{12}G_{21}$) since the cross-coupling between the ith input and the jth output is neglected during the design process. Figure 1(a) can also be rearranged as shown in Fig. 1(b). Notice that while the controller C_2 is designed for the nominal subsystem model G_{22}, the cross-coupling terms (G_{12} and G_{21}) and the controller C_1 introduce an additional path from u_2 to y_2. Therefore, the combined model from u_2 to y_2 is

$$G_2 = G_{22} + \Delta_{A1} \tag{2}$$

where $\Delta_{A1} = G_{21}C_1G_{12}/\left(1 - C_1G_{11}\right)$ is the additive error introduced by C_1. If the local control system designed for G_{22} is not robust to the modeling error introduced by C_1, then the coupled system will be unstable. Therefore, decentralized control requires robust local controllers.

Robust stability can be expressed in terms of the gain margin, which is a measure of the system's tolerance to multiplicative error. Therefore, it is beneficial to rewrite Eq (2) as

$$G_2 = G_{22}\left(1 + \Delta_{M1}\right) \tag{3}$$

where $(1 + \Delta_{M1})$ is the multiplicative error, and the multiplicative uncertainty Δ_{M1} is defined as $\Delta_{M1} = \Delta_{A1}/G_{22}$. In this example,

$$\Delta_{M1} = \left(\frac{G_{21}G_{12}}{G_{11}G_{22}}\right)\left(\frac{C_1G_{11}}{1 - C_1G_{11}}\right). \tag{4}$$

Notice that the first term in parentheses provides a measure of the diagonal dominance of the plant. This term will be large if the plant is not diagonally dominant (ie the product of the cross-coupling terms is large with respect to the product of the diagonal terms). The second term in Eq (4) is the complementary sensitivity function, T_1. To maintain robust

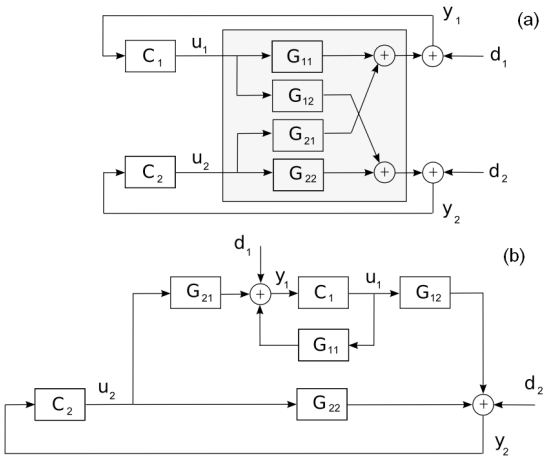

Figure 1: (a) Standard block diagram for a two-channel decentralized control system; (b) Rearranged diagram highlighting the additive error.

stability, the control system designed for subsystem 2 must be robust in the frequency bands where the plant is not diagonally dominant and at frequencies where T_1 is large. Since decentralized control units are designed completely independently, there is no way of knowing the cross terms or the complementary sensitivity function in advance. However, we do have access to the local control models, G_{11} and G_{22}. Notice in Eq (4) that the multiplicative uncertainty is inversely proportional to the product of the diagonal terms. Therefore, the uncertainty tends to be large at the zeros of G_{11} and G_{22}. As a result, it is often advantageous to penalize control effort at the zeros of the local control model. The following section explains how a frequency-shaped LQG design can be used to achieve this goal.

3 Linear quadratic Gaussian (LQG) control

LQG control is an optimal control strategy that uses minimum variance state estimates with an optimal state regulator. While the state regulator has guaranteed stability margins, the LQG controller can have arbitrarily poor stability margins due to errors in the state estimates [3]. Therefore, frequency shaping and loop transfer recovery are both commonly used to improve the performance and stability of the design.

Frequency-shaped designs can be generated by shaping the state regulator, the stochastic estimator, or both [4]. For instance, one way to shape the regulator is to augment the plant model with filter dynamics that produce additional frequency-weighted outputs. The frequency-shaped outputs are then included in the cost function and the optimal feedback gain matrix is calculated to minimize this new function. Therefore, we can penalize the control effort at the zeros of the local control model by augmenting the plant with low-order band-pass filters that generate an additional output u_f. The cost function can then be expressed in terms of this new output as

$$J = \int_0^\infty \left(q_1 y^2 + q_2 u_f^2 + r u^2\right) dt \qquad (5)$$

where q_1 is the original output weighting term, q_2 weights the new output, and r weights the frequency independent control effort u. In this case, the effective effort penalty at each frequency will be the sum of the frequency dependent and independent terms [5].

While it is often useful to penalize control effort using frequency shaped designs, modeling error is not restricted to the zeros of the local control models. Therefore it is not always possible to penalize control effort and improve robustness without significant performance penalties. Loop transfer recovery provides an alternative that can often be used to improve robustness without making the controller overly conservative.

4 Loop transfer recovery (LTR)

As discussed earlier, the guaranteed stability margins associated with full-state feedback are lost when the estimator is introduced. In response to this problem, loop transfer recovery (LTR) was developed by Doyle [6] to asymptotically "recover" the properties of the full-state feedback design. Essentially, LTR modifies the estimator such that the LQG system inherits the robustness of the state regulator. As the name implies, the robustness of the regulator is recovered by making the LQG loop transfer function approach that of the state regulator [7]. Recovery is achieved by injecting fictitious noise at the plant input. If the plant is stabilizable, completely observable, time-invariant and also minimum phase, then the LQG design will asymptotically recover the characteristics of the state regulator as the amplitude of the fictitious input noise becomes arbitrarily large [4].

Unfortunately, full loop transfer recovery is only guaranteed if the system is minimum phase. This is because full recovery relies on pole-zero cancelations. Note that even if the plant $G = C(sI - A)^{-1}B$ is not minimum phase, the continuous-time LQR loop transfer function, $L_{LQR} = -K(sI-A)^{-1}B$ is minimum phase. This explains the attractive gain and phase margins associated with the full state design. However, if G is not minimum phase, then full recovery would imply that the compensator uses right-half-plane poles to cancel the right-half-plane zeros. Since no stabilizing compensator can use unstable poles to cancel right-half-plane zeros, full recovery is only possible if the system is minimum phase. Unfortunately, noncollocated transducers often yield right-half plane zeros. Therefore, full recovery is rarely possible. Luckily, partial loop recovery is often adequate to account for plant uncertainty. Partial recovery is achieved by increasing the amplitude of the fictitious input noise until maximum robustness is achieved. Another option is to use frequency-shaped recovery. This enables different performance/robustness trade-offs in different frequency bands [8].

Although loop recovery can be effective, it is limited to recovering the characteristics of the state regulator. Therefore, the approach is only suitable if the underlying LQR design is robust. As a result, a two-step approach is advocated. First, the effort penalty is shaped to ensure the LQR design is sufficiently robust. This is accomplished by limiting control authority at the zeros of the local control model. As discussed earlier, this typically improves the robustness of the design without significant reductions in achievable performance. Next, frequency-shaped loop recovery is used in frequency bands where the interaction between controllers

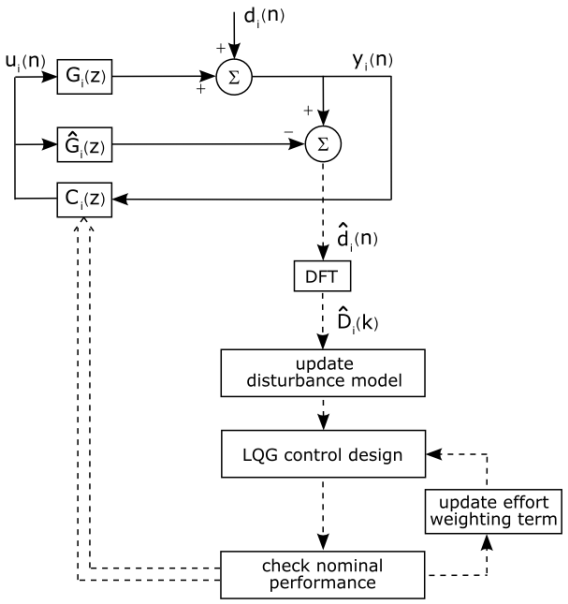

Figure 2: A diagram of the iterative control strategy.

limits achievable performance. Unfortunately, it is often difficult to accurately predict the frequency bands where loop recovery is required *a priori*. Therefore the following section describes the concept of iterative loop recovery.

5 Iterative loop recovery

The iterative approach described in this paper incorporates loop recovery in a simple iterative loop. The strategy is depicted in Fig. 2 using $G_i(z)$ to represent the physical system and $d_i(n)$ as the disturbance. The subscript i denotes that the control strategy is implemented on the i^{th} subsystem. The controller is designed using an internal plant model $\hat{G}_i(z)$, which is used to generate an estimate of the disturbance $\hat{d}_i(n)$ at each time step. Although this resembles an internal model control structure [9], the input to the online controller $C_i(z)$ is the observed error signal $y_i(n)$ instead of the disturbance estimate. While the diagram only depicts one control unit, the control strategy is implemented simultaneously on each subsystem.

The control strategy can be divided into two processes: a real-time process that occurs on a sample-by-sample basis, and an update procedure that occurs much less frequently. The steps involved in the update procedure are connected by the dashed lines in Fig. 2. Essentially, an LQG controller is updated periodically using a new effort weighting term and disturbance model. The disturbance model is calculated from the discrete Fourier transform of the disturbance estimate, $\hat{D}_i(k)$. Once the disturbance model and effort weighting term are updated, the LQG controller is redesigned. If the design satisfies control effort and performance considerations, then the online controller $C_i(z)$ is updated. The entire process is repeated until the control effort approaches predefined limits, or until subsequent designs fail to improve control performance.

While it might not be obvious at first, this strategy relies on frequency shaped loop recovery. Loop recovery is exploited by increasing the amplitude of the disturbance model. Although changes in the disturbance model introduce fictitious noise at the plant output, output noise can also be represented as appropriately shaped input noise if the system only has one input and one output. Therefore, increasing the amplitude of the disturbance model is used to improve the robust stability and performance of the control system by partially recovering the characteristics of the LQR design.

Recall that the proposed control strategy uses an internal model to generate the disturbance estimate $\hat{d}_i(n)$. If the plant model is perfect, then the estimate will accurately track changes in the true disturbance. However in frequency bands where $\hat{G}_i(z) \neq G_i(z)$, the amplitude of the disturbance estimate could be larger or smaller than the actual disturbance. While increasing the amplitude of the disturbance model typically improves robustness by exploiting loop recovery, decreasing the amplitude of the model can make the design more sensitive to modeling error. Therefore the disturbance model is updated by taking the maximum of the current disturbance estimate and the previous disturbance model on a frequency-by-frequency basis. In other words, the model is only changed if the magnitude of the disturbance estimate exceeds the magnitude of the previous disturbance model.

In summary, the first step in the design process is to identify an accurate subsystem model. The effort weighting term is then shaped to penalize control effort at the zeros of the open-loop system. Shaping the effort term limits excessive compensator gain and improves the stability margins of the LQR design. Next, the measured response is used to generate an initial model of the disturbance. The disturbance model is then used to calculate the optimal state estimator. If the initial LQG controller meets minimum stability requirements, then the controller is applied. The update procedure is implemented by updating the disturbance model to account for changes introduced by neighboring control loops. In other words, the disturbance model is updated to make the system more robust in frequency bands where modeling error is excessive. Next, the LQG controller is redesigned using the new disturbance model and a more aggressive effort weighting model. The new controller is evaluated based on control effort and performance criteria. If the design is acceptable, then the online controller is updated. The process is then repeated until the control effort approaches predefined limits, or until subsequent designs fail to improve control performance. Additional details pertaining to this approach can be found in Schiller [10].

6 Experimental Setup

The control strategy was evaluated using real-time experiments performed on a flat aluminum skin-stringer panel. The $1.17\,\mathrm{m} \times 1.17\,\mathrm{m} \times 0.00127\,\mathrm{m}$ panel, shown in Fig. 3, was segmented into 10 approximately equal size bays with nominal dimensions of $0.45\,\mathrm{m} \times 0.19\,\mathrm{m}$. For logistical reasons, transducers were only attached to the two bays shown in Fig. 4. The remaining bays were covered with lead-vinyl. For these tests, the stiffened panel was mounted in the transmission loss window in the Structural Acoustic Loads and Transmission (SALT) facility at NASA Langley Research Center. The panel was driven by a broadband acoustic disturbance, while radiated sound power was estimated using a discrete array of structural measurements. In particular, a 5

Figure 3: Photograph of the stiffened aluminum test panel.

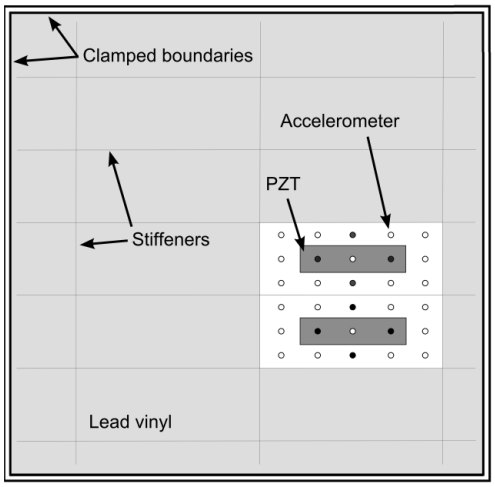

Figure 4: Diagram of the front of the panel.

$\times$ 6 grid of miniature accelerometers was used to measure the structural response of the two bays. Acoustic power was then estimated using radiation modal expansion [11]. Data acquisition and control were implemented using xPC Target. Since the response was sampled at 3 kHz, 1 kHz anti-aliasing prefilters and smoothing postfilters were used on all inputs and outputs.

The control transducers consisted of surface-mounted piezoceramic patches and accelerometers, as shown in Fig. 4. Specifically, 0.07 m by 0.29 m piezoelectric actuators were mounted in the center of each bay, and four accelerometers were located in a diamond pattern around each actuator. When integrated, the summed response from the accelerometers provided an estimate of the volume velocity of each bay. This transducer configuration was selected based on the controller/transducer complexity work performed by Gibbs et al. [12].

7 Results and Discussion

Initially input/output data was acquired to characterize each subsystem. This was accomplished by driving the PZT actuators with broadband random noise while recording the response of each sensor. The observer/Kalman filter identification (OKID) algorithm [13] was then used to compute 75 th order state-space models of each subsystem. Conservative initial LQG controllers were then designed and implemented on each subsystem. The controllers were updated independently using the procedure described in the previous section. In particular, 60 th order disturbance models were updated based on the closed-loop response, while the effort penalty was slowly reduced. This procedure was implemented iteratively until the control system converged.

The power spectra of the volume velocity estimates acquired on the upper bay are shown in Fig. 5. The open-loop response is shown with the thin blue line, the initial closed-loop performance is indicated with the thick red line, and the final closed-loop response is shown by the dotted black line. The poor initial performance at 145 Hz was due to the interaction between the local controllers. As the controllers were updated, the amplitude of the disturbance model increased around 145 Hz. This significantly improved the performance of subsequent designs. The final design reduced the 145 Hz peak by more than 10 dB and achieved a 4 dB integrated reduction from 50 to 600 Hz. Since the same trends were also observed on the lower bay, those results are not shown here.

The total radiated sound power from both bays is shown in Fig. 6. The final design achieved a 2.7 dB integrated reduction from 50 to 600 Hz, as shown by the thick red line. Spillover above 700 Hz was due to the fact that the integrated and summed accelerometers provided a poor estimate of volume velocity at high frequencies. When a more accurate estimate of radiated sound power was used for control, the system achieved 12 dB peak reductions and a 3.6 dB integrated reduction in radiated sound power. In addition, the high frequency spillover from 600 to 800 Hz was reduced as shown by the dotted black line in Fig. 6. In this case, the control system had access to radiated sound power estimates generated in real time using the radiation modal expansion technique [11].

8 Concluding Remarks

Decentralized controllers introduce unavoidable errors due to the unmodeled coupling between subsystems. In particular, the modeling error can be expressed as the product of the complementary sensitivity function for the neighboring control loop multiplied by a term that quantifies the diagonal dominance of the plant. While closed-loop performance can often be improved by penalizing control effort at the zeros of the local control models, that approach is not always sufficient. Therefore the concept of loop transfer recovery was used to develop a time-varying strategy. This iterative strategy was validated using real-time control experiments performed on a structural-acoustic system with poles close to the stability boundary, non-minimum phase zeros, and unmodeled dynamics. Experimental results showed that updating the disturbance model based on closed-loop system measurements improved the robust stability and performance of the control system. In particular, the iterative control system achieved 12 dB peak reductions and a 3.6 dB integrated reduction in radiated sound power from two adjacent aircraft-style bays.

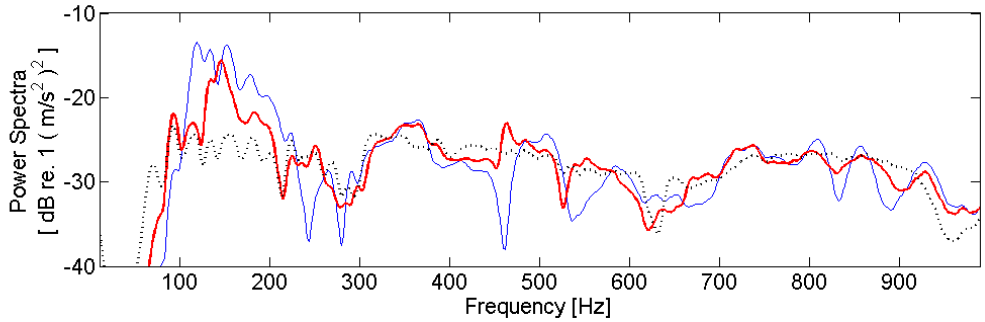

Figure 5: The power spectra of the measured response on the upper bay before control (thin blue line), using the initial controller (thick red line), and using the final design (dotted black line).

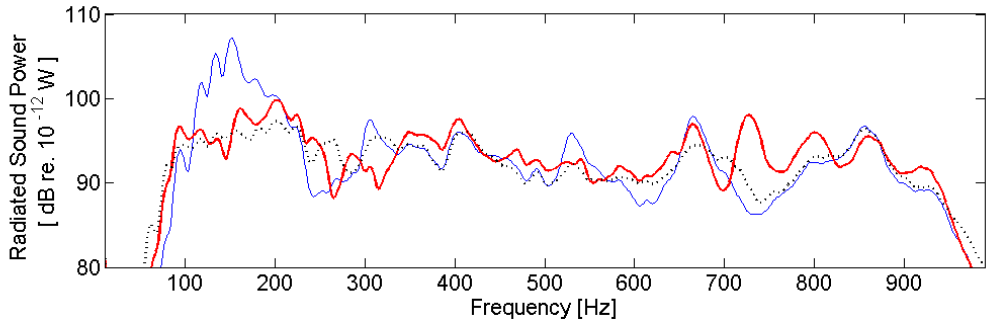

Figure 6: The total radiated sound power from the two bays before control (thin blue line), using the standard control system with summed accelerometers (thick red line), and using a more accurate radiated sound power estimate (dotted black line).

References

[1] R.H. Cabell, D.E. Cox, G.P. Gibbs, "Interaction metrics for feedback control of sound radiation from stiffened panels", *Proceedings of the 44th AIAA/ASME/ASCE/AHS Structures, Structural Dynamics, and Material Conference* 7-10 April, Norfolk, Virginia (2003)

[2] G.P. Gibbs, R.H. Cabell, "Simultanteous active control of turbulent boundary layer induced sound radiation from multiple aircraft panels", *Proceedings of the 8th AIAA/CEAS Aeroacoustics Conference* 17-19 June, Breckenridge, Colorado (2002)

[3] J.C. Doyle, "Guaranteed margins for LQG regulators", *IEEE Trans. Automatic Control* AC-23:756-757 (1978)

[4] B.D.O. Anderson, J.B. Moore, *Optimal Control: Linear Quadratic Methods*, (Prentice Hall, New Jersey, 1990)

[5] R.H. Cabell, M.A. Kegerise, D.E. Cox, G.P. Gibbs, "Experimental feedback control of flow-induced cavity tones", *AIAA J.* 44:1807-1815 (2006)

[6] J.C. Doyle, G. Stein, "Robustness with observers", *IEEE Trans. Automatic Control* AC-24:607-611 (1979)

[7] R.R. Bitmead, M. Gevers, V. Wertz, *Adaptive Optimal Control: The Thinking Man's GPC*, (Prentice Hall, New Jersey, 1990)

[8] G. Stein, M. Athans, "The LQG/LTR procedure for multivariable feedback control design", *IEEE Trans. Automatic Control* AC-32:105-114 (1987)

[9] M. Morari, E. Zafiriou, *Robust Process Control*, (Prentice Hall, New Jersey, 1989)

[10] N.H. Schiller, "Decentralized control of sound radiation from periodically stiffened panels", PhD thesis, Virginia Tech, Blacksburg, Virginia (2007)

[11] G.P. Gibbs, R.L. Clark, D.E. Cox, J.S. Vipperman, "Radiation modal expansion: Application to active structural acoustic control", *J. Acoust. Soc. Am.* 107:332-339 (2000)

[12] G.P. Gibbs, R.H. Cabell, J. Juang, "Controller complexity for active control of turbulent boundary layer noise from panels", *AIAA J* 42,1314-1320 (2004)

[13] J. Juang, *Applied System Identification*, (Prentice Hall, New Jersey, 1994)